Characterization of Musa Paradisiaca Activated Carbon Supporting Iron Nanoparticles, after Adsorption of Hydrogen Sulphide (H2S) from Biogas on a Fixed Bed Column

GBANGBO Rémis KONAN (konanremis@gmail.com)
Institut National Polytechnique Félix Houphouët-Boigny
KOUAKOU Rodrigue ADJOUMANI
Université Nangui Abrogoua
EHOUMAN DONATIEN
Université Nangui Abrogoua
Benjamin YAO
Institut National Polytechnique Félix Houphouët-Boigny
Gonézié Vanessa-Edwige GOLI LOU
Institut National Polytechnique Félix Houphouët-Boigny
Briton Bi Henri GOUESSE
Institut National Polytechnique Félix Houphouët-Boigny
Tougnon Zéphirin GNABOA
Institut National Polytechnique Félix Houphouët-Boigny
Koffi Née Alphonsine Badou Affoua BAH
Institut National Polytechnique Félix Houphouët-Boigny
Mahamane Nassirou AMADOU KIARI
Institut National Polytechnique Félix Houphouët-Boigny

Research Article

Keywords: Biogas, H2S, adsorption, activated carbon, Musa Paradisiaca,

Posted Date: February 14th, 2023

DOI: https://doi.org/10.21203/rs.3.rs-2577769/v1

Abstract

In this study, the characteristics of Musa Paradisiaca (MP) iron-funtionalysed activated carbon (AC) after adsorption of H_2S from biogas were demonstrated. The AC was chemically impregnated with potassium hydroxide (KOH) and then carbonised at a temperature of 500°C for 3 hours for activation. The activated carbon was then functionalized with iron oxide (Fe_2O_3) and labelled BANK-Fe. The H_2S adsorption test was performed on a fixed bed column. The biogas flow rate was 1 $L.min^{-1}$. with 25% water (w/w) added. This test resulted in an adsorption capacity of 9.86 mgH_2S.g-1 after a saturation time of 615 minutes. This was satisfactory for the purposes of biogas treatment. The present work is a follow-up to the adsorption tests already carried out. The analyses on the functionalized activated carbon sample after adsorption underwent a physical and chemical change. The surface morphology was modified: the more or less homogeneous asperities of the BANK-Fe (before adsorption) gave way to a relatively more amorphous form. Sulphur elements were detected in the sample after adsorption, in contrast to the starting sample. This confirms the adsorption of H_2S from the biogas. Oxygen and Iron in BANK-Fe decreased by 39.49% and 94.16% respectively in atomic concentration, which proves that they reacted and played a role in the H_2S adsorption mechanism. In addition, the microporosity decreased by 35.71%: the iodine value decreased from 1065.96 $mg.g^{-1}$ to 685.26 mg.g-1. This indicates that part of the pores, in particular the micropores, was occupied by the pollutants during the adsorption of the biogas.

1. Introduction

As a result of a number of factors, including the very rapid post-pandemic economic recovery, tensions in the energy market emerged in 2021. The situation worsened dramatically after Russia invaded Ukraine in February 2022, creating a global energy crisis. Gas prices have reached record levels, leading to record electricity prices in some markets. This situation threatens people's well-being, both economically and environmentally [1]. To remedy this, previous and recent work has focused on finding alternative energies to reduce dependence on fossil fuels [2]. This research is therefore aimed at finding other sources of so-called renewable energy, which are considered inexhaustible on a human timescale and generate little or no waste or polluting emissions. Among these renewable energies, biogas remains a solution of choice for developing countries to make the energy transition [3], in view of the relatively low production cost. Biogas is a gaseous mixture that is obtained by degradation of organic waste under anaerobic conditions. This degradation is carried out by specific microorganisms under anaerobic conditions [1]. The main compound sought in biogas is methane (CH_4) because it can be combusted for heat and/or electricity [2]. Indeed, the calorific value of biogas depends on its CH_4 content: the higher the CH_4 content, the higher its calorific value [4]. Whether for direct combustion or cogeneration, it is important to go through an H_2S purification step. This prevents damage to equipment and environmental pollution from hydrogen sulphide emissions [5]. Indeed, H_2S is extremely toxic: It can cause damage to the nervous system, even in low concentrations [6]. It is toxic to microorganisms, and is corrosive to concrete and steel [6]. In addition to being malodorous, H_2S is also a source of acid rain: this makes it a significant pollutant of the air and the environment [6]. Among the technologies used in H_2S removal from biogas streams is adsorption on activated carbons (AC) from lignocellulosic feedstocks. This is a process safe, sustainable, reliable, highly efficient, and an environmentally sound [5, 7–10]. In a recent work, we used activated carbons based on plantain peel for the adsorption of H_2S from a real biogas. The AC was chemically

impregnated with potassium hydroxide (KOH) and then carbonised at a temperature of 500°C for 3 hours for activation. Subsequently the activated carbon was functionalised with iron oxide (Fe2O3). This functionalized activated carbon was named BANK-Fe (Banana peel carbon activated with potassium hydroxide and functionalized with iron nanoparticles). The H_2S adsorption test was performed on a fixed bed column. The biogas flow rate was 1 $L.min^{-1}$. To allow chemisorption of H_2S [11], 25% water (w/w) was added to the filter media. This test resulted in an adsorption capacity of 9.86 $mgH_2S.g^{-1}$ after a saturation time of 615 minutes. After adsorption, it is only logical to expect a physical and/or chemical change in the activated carbon. In recent work, Choudhury and Lansing [12], through SEM elemental mapping showed uniform distribution of sulfur on the biochar surface. Our work aims to highlight the modification of the microporosity by analysing the variation of the iodine index. Moreover, we want to highlight the modification of the surface morphology and the chemical elements of BANK-Fe.

2. Materials And Methods

2.1. Production parameters of functionalized activated carbon and H_2S adsorption test.

The conditions for impregnation, carbonisation and functionalisation of activated carbon are summarised in Table 1. The main production factors are: impregnation rate and duration, carbonisation duration and temperature. The concentrations of KOH and Fe_2O_3 used were 500 ppm and 5000 ppm respectively.

Tableau 1: Production parameters for functionalized activated carbon

KOH Impregnation		Carbonization		Fe_20_3 functionalization			
Rate	Duration	Temperature	Duration	Rate	Duration of impregnation	Carbonisation temperature	Duration of carbonisation
0.3 $g.mL^{-1}$	12h	500°C	3h10	$5.10^{-2}g.mL^{-1}$	2h30	300°C	50 min

BANK-Fe functionalized activated carbon was used for the adsorption of H_2S from biogas. The H_2S adsorption test was performed on a fixed bed column. The biogas flow rate was 1 $L.min^{-1}$. with 25% water (w/w) added. This test resulted in an adsorption capacity of 9.86 $mgH_2S.g$-1 after a saturation time of 615 minutes.

2.1. Iodine index value

The iodine value (Id) expressed in mg/g was calculated by applying the expression: [13] and cited by Gbangbo et al., (2023).

$$I_d = \frac{126.9.N.(V_b - V_s).(\frac{10}{15})}{m_c}.100 \text{ (Eq. 1)}$$

Vb: volume in mL of a 0.1 N sodium thiosulphate solution, poured in a test without AC, Vs: volume in mL of 0.1 N sodium thiosulphate solution poured in the test with adsorbent, N: normality of solution sodium thiosulphate

solution in (eq.g/L), 126.9: atomic mass of iodine, mc is the mass of the AC in (g). A 0.05 g of AC was used.

2.2. pH

The determination of pH was carried out using the method described by Shang et al. (2016). 1 g of activated carbon is added to 50 mL of distilled water. The mixture was stirred for 30 minutes using a bar magnet. The pH of the filtered solution was then measured.

2.3. Scanning Electron Microscopy (SEM) coupled with energy dispersive spectroscopy (EDS) of activated carbon

Pour connaître la morphologie du charbon actif, la Microscopie électronique à balayage a été utilisée. Un spectrophotomètre de marque Hiro SH400 M a été utilisé à cet effet. Quant à la composition chimique des éléments et leur cartographie, la méthode analytique EDS a été utilisé. L'appareil utilisé à cet effet est de marque BRUCKER, modèle XFlash 30/100. Ces analyses se sont effectuées au laboratoire central de Man, Côte d'Ivoire.

3. Results And Discussion

3.1. Indice d'iode

The iodine value decreased by 35.71% after biogas purification (Table 2). In addition, Chekem [15] notes that, as a general rule, the adsorbent with the highest iodine value will have the largest specific surface area. Thus, this decrease in microporosity can be explained by the occupation of part of the micropores by biogas pollutants with small molecules (less than or equal to 2 nm).

Table 2
Change in iodine value of BANK-Fe (before and after H_2S adsorption)

Paramètres	Avant adsorption	Après adsorption
Iodine index value ($mg.g^{-1}$)	1065.96	685.26

Furthermore, several researchers have pointed out that the iodine value and the specific surface area move in the same direction [16–18]. For exemple, Asadullah et al. [16] obtained a variation from 724 to 360 $m^2.g^{-1}$ for the specific surface, and from 573 to 255 $mg.g^{-1}$ for the iodine index.

3.2. Surface morphology and chemical elements

The modification of the microporosity leads to a change in the surface morphology, as shown in Fig. 1 and Fig. 2. There is a notable change in the appearance of the activated carbon. The more or less homogeneous asperities perceptible on Fig. 1 (before adsorption) have given way to a relatively more amorphous form (Fig. 2).

Le changement d'aspect mis en évidence par le MED s'accompagne d'un changement dans la composition des éléments chimiques du CA (tableau 3). Par exemple, on retrouve l'élément soufre (S) dans l'échantillon après adsorption. Ce qui n'est pas le cas avant adsorption. Ce composé (soufre) provient sans doute du H_2S contenu dans le biogaz.

The reactions leading to the formation of elemental sulfur are described by Eq. 2 where Species (H_2S and O_2) adsorbed on free sites of the solid can then react together, leading to the formation of elemental sulfur and hydroxide ions. [11]

$H_2S^-_{ads} + O_{ads} \rightarrow S_{ads} + OH^-$ (Eq. 2)

The decrease in iron (Fe) content can be attributed to the oxidation reaction involving metal ions. This is because the main H_2S removal mechanism was shown to be the impregnated iron (as Fe_2O_3) directly reacting with the gaseous H_2S dissolved in the water film [12].

Table 3
Physical and Chemical characteristics of BAN-K and BANK-Fe ACs

Parameters	adsorbents	
	Before adsorption	After adsorption
C (%)	62.25	89.67
O (%)	9.47	5.73
K (%)	-	3.55
Fe (%)	10.11	0.59
S (%)	0.00	1.11
pH	9.67	10.22

The oxygen content of the AC decreased by 39.50%. This confirms that some of this oxygen was used up in the adsorption mechanism [19, 11]. Indeed, Coppola and Papurello [20] have shown that during the adsorption of H_2S from biogas, the adsorption capacity of the AC decreases as the oxygen content decreases. On the other hand, there is no major change in the hydrogen potential (pH). The surface of the AC was basic before adsorption (9.67) and remained basic after adsorption (10.22). This can be justified by the fact that the charcoal was initially impregnated with a strong base (potassium hydroxide) before carbonisation. The spectrum of the chemical elements of the AC after adsorption and their mapping are presented in Fig. 3 and Fig. 4.

4. Conclusion

The MP activated carbon sample functionalized with iron oxide underwent morphological and chemical changes. These changes in appearance and chemical constitution appeared after the adsorption of H2S from biogas. Clearly, the appearance of elemental sulphur in the chemical matrix of the AC shows that the H2S from the biogas was effectively adsorbed via chemisorption and physisorption mechanisms. This is reflected in the variation of the atomic concentrations of oxygen and iron in the AC. The knowledge of the nature of the chemical elements is necessary for the choice of the regeneration process. Regeneration of AC is an act that restores the adsorption capacity of AC that was lost during saturation. Regeneration can therefore allow the activated carbon to be used for a longer period of time. This offers economic and environmental benefits. The preparation of the carbon has a cost, so regeneration is a way of reducing the additional expense of producing

new carbon. Based on our results, it is possible to consider biological desulfurisation of AC, using sulfur reducing bacteria.

Declarations

Declaration of interests

The authors declare that they have no known competing financial interests or personal relationships that could have appeared to influence the work reported in this paper.

The authors declare the following financial interests/personal relationships which may be considered as potential competing interests:

References

1. N. N. Zulkefli, M. S. Masdar, W. N. R. Wan Isahak, J. Md Jahim, S. A. Md Rejab, et C. Chien Lye, « Removal of hydrogen sulfide from a biogas mimic by using impregnated activated carbon adsorbent », *PLoS ONE*, vol. 14, n° 2, p. e0211713, févr. 2019, doi: 10.1371/journal.pone.0211713.
2. N. Ho, « Modeling Hydrogen Sulfide Adsorption by Activated Carbon made from Anaerobic Digestion By-Product ». Department of Chemical Engineering and Applied Chemistry University of Toronto, 2012.
3. H. Sawalha, M. Maghalseh, J. Qutaina, K. Junaidi, et E. R. Rene, « Removal of hydrogen sulfide from biogas using activated carbon synthesized from different locally available biomass wastes - a case study from Palestine », *Bioengineered*, vol. 11, n° 1, p. 607-618, janv. 2020, doi: 10.1080/21655979.2020.1768736.
4. A. Pertiwiningrum, T. Rhema, M. A. Wuri, N. A. Fitriyanto, et A. E. Tontowi, « The effect of chemical activation of biochar on biogas purification », *IOP Conf. Ser.: Earth Environ. Sci.*, vol. 1108, n° 1, p. 012032, nov. 2022, doi: 10.1088/1755-1315/1108/1/012032.
5. E. Surra, M. Costa Nogueira, M. Bernardo, N. Lapa, I. Esteves, et I. Fonseca, « New adsorbents from maize cob wastes and anaerobic digestate for H2S removal from biogas », *Waste Management*, vol. 94, p. 136-145, juill. 2019, doi: 10.1016/j.wasman.2019.05.048.
6. G. Shang, Q. Li, L. Liu, P. Chen, et X. Huang, « Adsorption of hydrogen sulfide by biochars derived from pyrolysis of different agricultural/forestry wastes », *Journal of the Air & Waste Management Association*, vol. 66, n° 1, p. 8-16, janv. 2016, doi: 10.1080/10962247.2015.1094429.
7. R. G. Ding, X. D. YAO, Z. H. ZU, G. Q. LU, et Z. YAN, « Effect of pore structure of activated carbon fibers on hydrogen adsorption », *Springer Science*, 2008.
8. I. Tchakala, L. M. BAWA, G. DJANEYE-BOUNDJOU, K. S. DONI, et P. NAMBO, « Optimisation du procédé de préparation des Charbons Actifs par voie chimique (H 3 PO 4) à partir des tourteaux de Karité et des tourteaux de Coton », *Int. J. Biol. Chem. Sci*, n° 6(1): 461-478, févr. 2012.
9. S. Kruaysawat, « Increasing adsorption efficiency of activated carbon for H2S removal by surface oxidation and metal addition ». Suranaree University of Technology, 2006.
10. F. Adib, A. Bagreev, et T. J. Bandosz, « Effect of Surface Characteristics of Wood-Based Activated Carbons on Adsorption of Hydrogen Sulfide », *Journal of Colloid and Interface Science*, vol. 214, n° 2, p. 407-415, juin 1999, doi: 10.1006/jcis.1999.6200.

11. V. Gasquet, « Epuration d'H2S du biogaz à partir de résidus de traitement thermique bruts et formulés : Comparaison des performances et compréhension des mécanismes d'adsorption ». Université de Lyon, 2021.
12. A. Choudhury et S. Lansing, « Adsorption of hydrogen sulfide in biogas using a novel iron-impregnated biochar scrubbing system », *Journal of Environmental Chemical Engineering*, vol. 9, n° 1, p. 104837, févr. 2021, doi: 10.1016/j.jece.2020.104837.
13. H. Koné, A. S. Assémian, T. Tiho, K. Adouby, K. B. Yao, et P. Drogui, « *Borassus aethiopum* activated carbon prepared for nitrate ions removal », *Journal of Applied Water Engineering and Research*, vol. 10, n° 1, p. 64-77, juill. 2021, doi: 10.1080/23249676.2021.1947400.
14. K. R. Gbangbo *et al.*, « Influence of Water Content on Hydrogen Sulfide Adsorption in Biogas Purification with Musa Paradisiaca Biochar », *Chemistry Africa*, févr. 2023, doi: 10.1007/s42250-023-00610-w.
15. T. C. Chekem, « Matériaux carbonés multifonctionnels à porosité contrôlée à partir des ressources végétales tropicales : application au traitement de l'eau par photocatalyse. », Université de Perpignan Via Domitia, PROMES – CNRS UPR 8521, 2017.
16. M. Asadullah, A. M. Rahman, A. M. Motin, et B. M. Sultan, « Adsorption studies on activated carbon derived from steam activation of jute stick char. », *J. surface Sci technol.*, vol. 23, n° 1-2 :, 2007.
17. G. Newcombe, J. Morrison, et C. Hepplewhite, « Simultaneous adsorption of MIB and NOM onto activated carbon. I. Characterisation of the system and NOM adsorption », *Carbon 40*, n° 40, p. 2135-2146, 2002.
18. K. C. Balogoun, L. M. Bawa, et M. Aina, « Préparation des charbons actifs par voie chimique à l'acide phosphorique à base de coque de noix de coco », *Int. J. Biol. Chem. Sci.*, vol. 9, n° 1, 2015.
19. R. Sitthikhankaew, D. Chadwick, S. Assabumrungrat, et N. Laosiripojana, « Effects of humidity, O2, and CO2 on H2S adsorption onto upgraded and KOH impregnated activated carbons », *Fuel Processing Technology*, vol. 124, p. 249-257, août 2014, doi: 10.1016/j.fuproc.2014.03.010.
20. G. Coppola et D. Papurello, « Biogas Cleaning: Activated Carbon Regeneration for H2S Removal », *Clean Technol.*, vol. 1, n° 1, p. 40-57, juin 2018, doi: 10.3390/cleantechnol1010004.

Figures

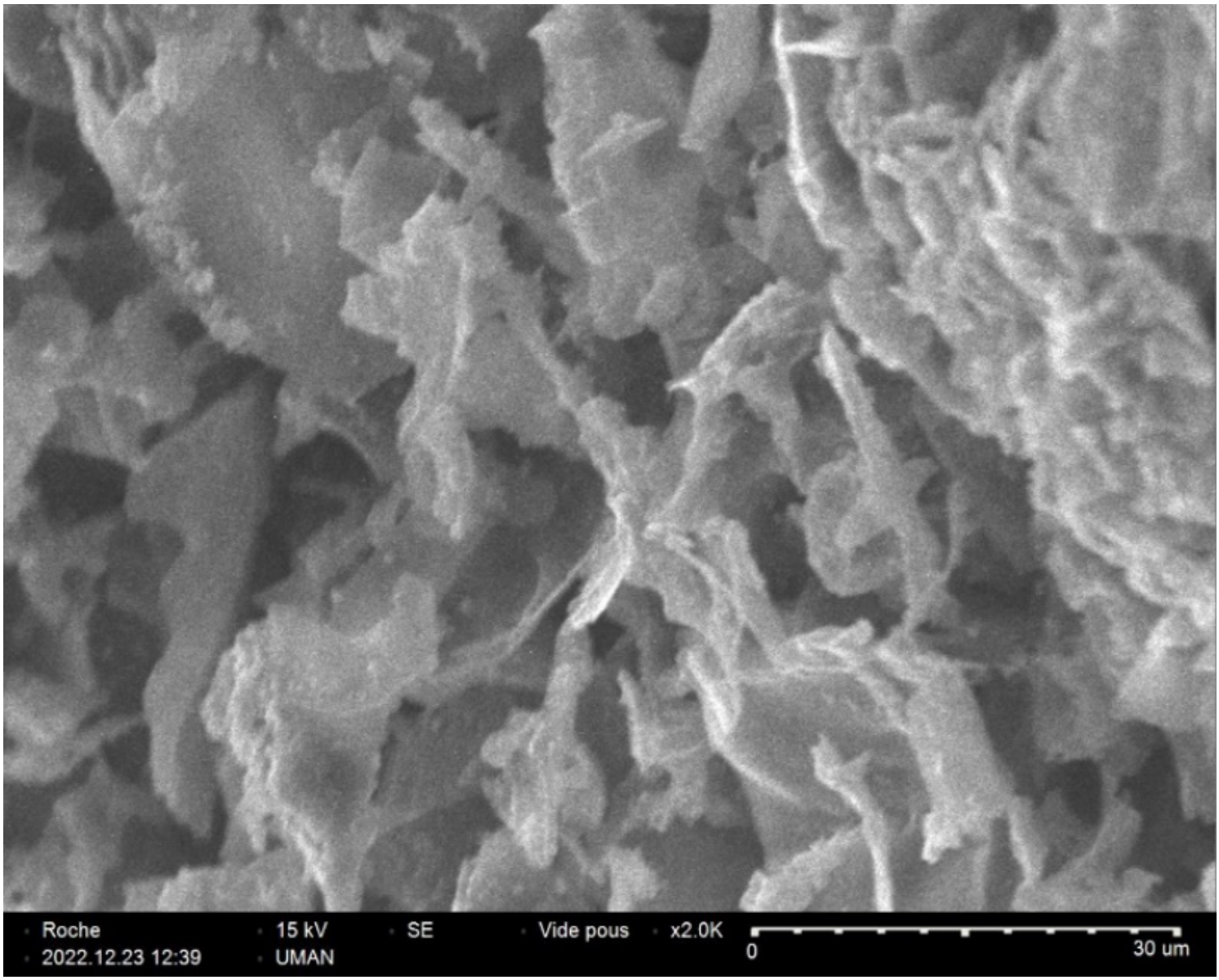

Figure 1

Morphology of activated carbon seen by scanning electron microscope (Before adsorption)

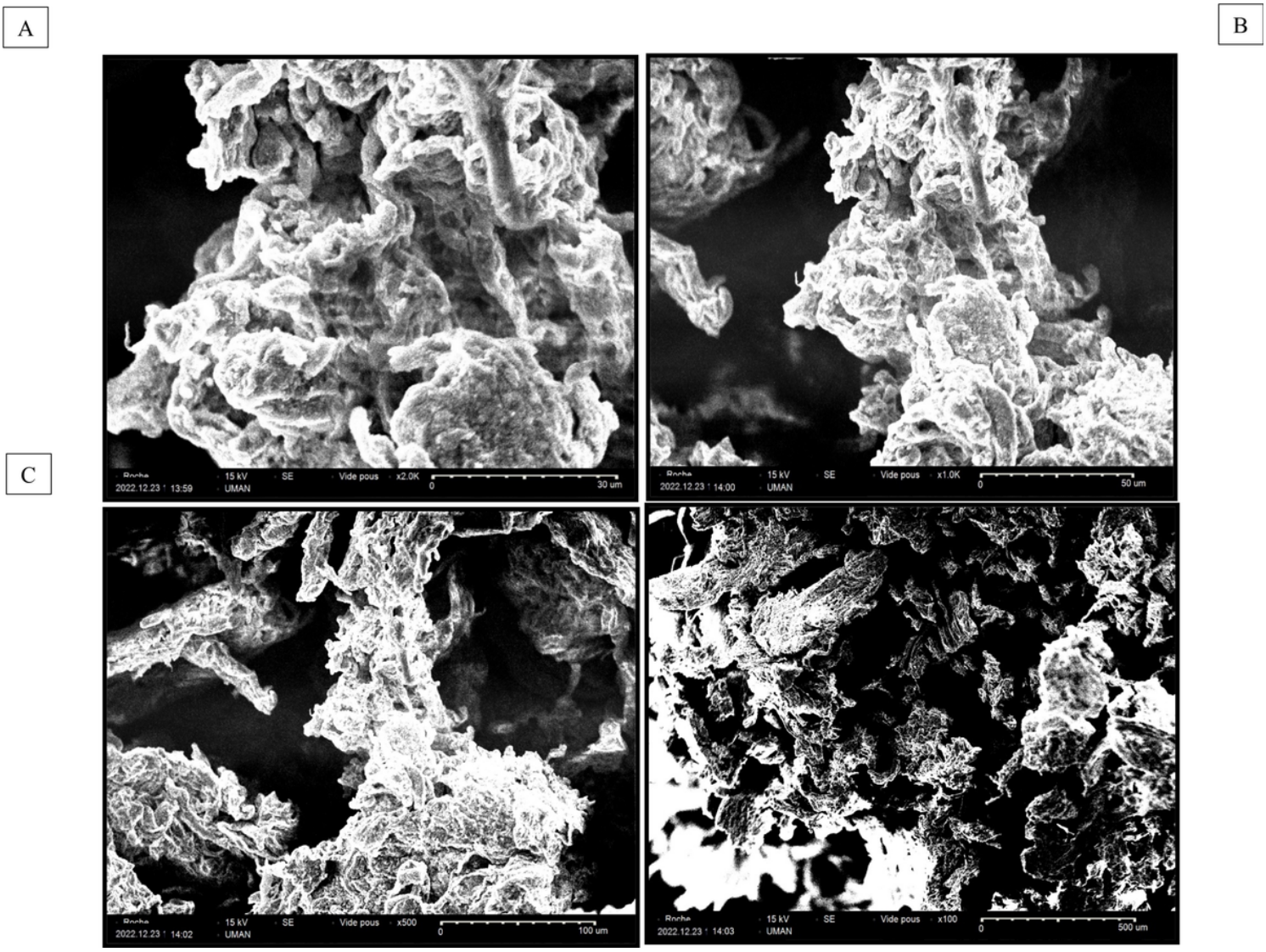

Figure 2

Morphology of activated carbon seen by scanning electron microscope (after adsorption)

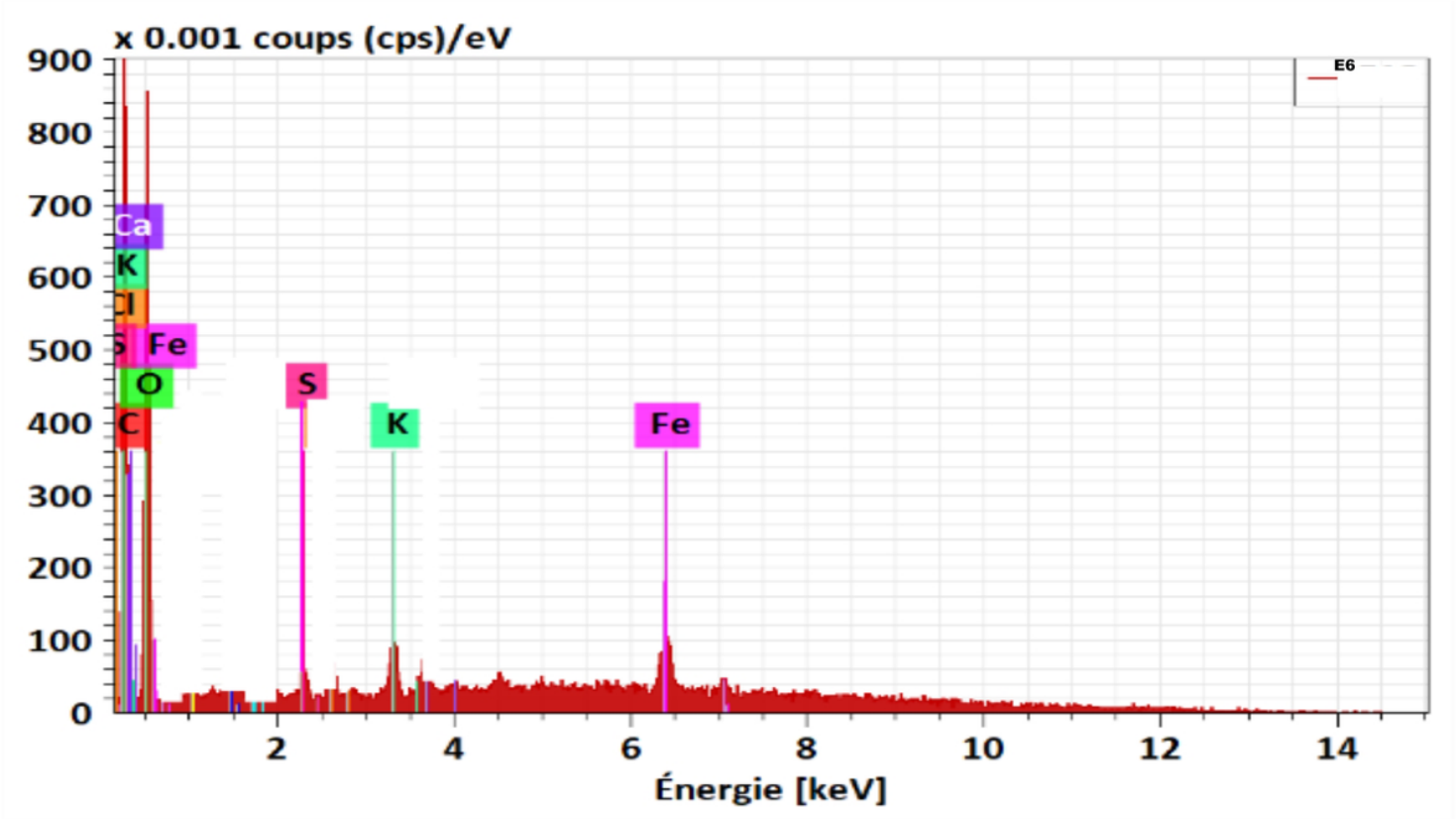

Figure 3

Spectre de l'échantillon après adsorption à 20 µmà l'aide de l'EDS

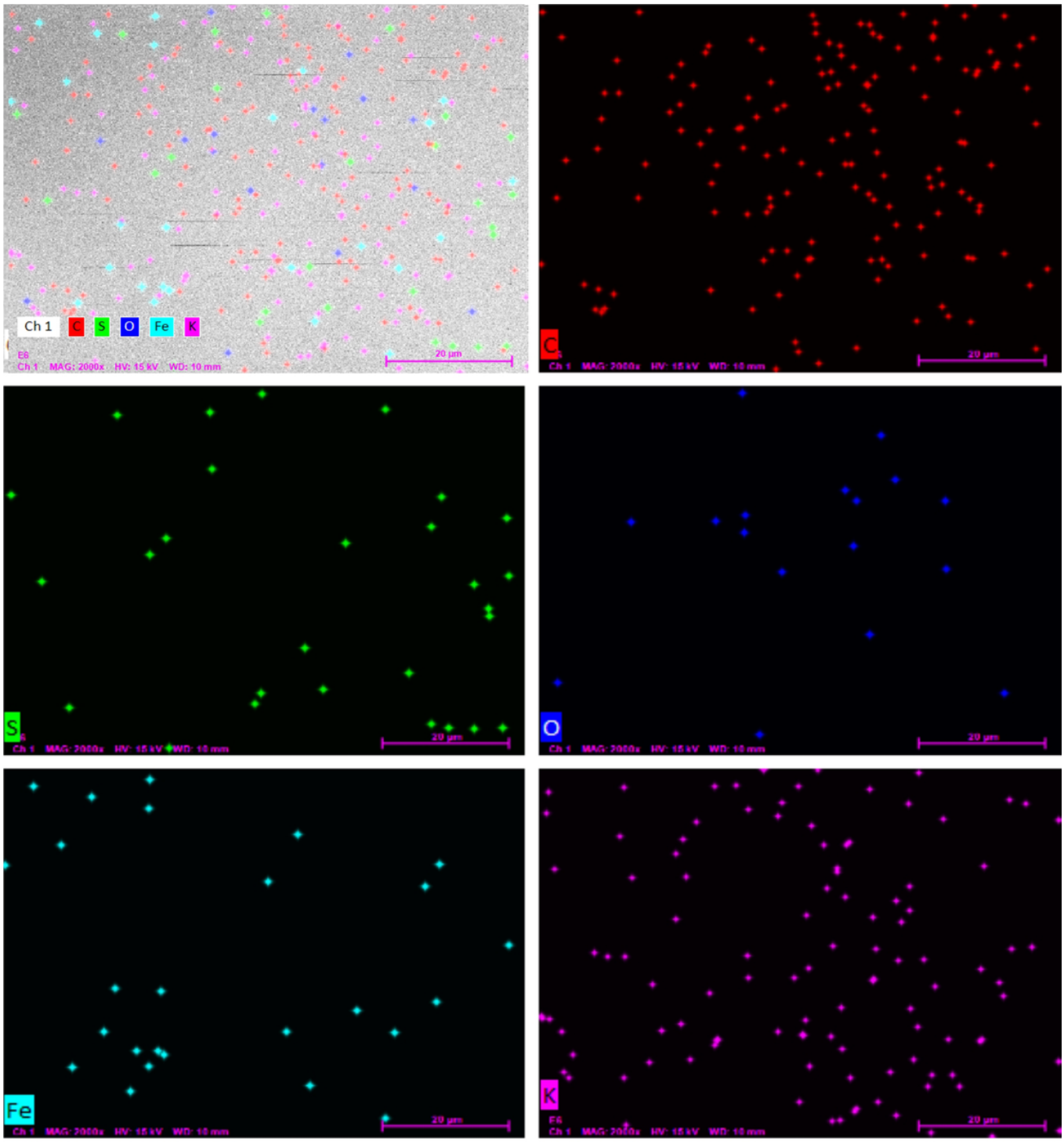

Figure 4

Mapping of the sample after adsorption at 20 µm using the BRUCKER EDS

Supplementary Files

This is a list of supplementary files associated with this preprint. Click to download.

- Highlights.docx